COTR AND SASE GENERATED BY COMPRESSED ELECTRON BEAMS*

A.H. Lumpkin, Fermilab, Batavia, IL U.S.A. 60510
R.J. Dejus and N.S. Sereno, Argonne National Laboratory, Argonne, IL U.S.A. 60439

Abstract

Observations of strongly enhanced optical transition radiation (OTR) following significant bunch compression of photoinjector beams by a chicane have been reported during the commissioning of the Linac Coherent Light Source (LCLS) accelerator and recently at the Advanced Photon Source (APS) linac. These localized transverse spatial features involve signal enhancements of nearly a factor of ten in the APS case at the 150-MeV and 375-MeV OTR stations. They are consistent with a coherent process seeded by noise and may be evidence of a longitudinal space charge (LSC) microbunching instability which leads to coherent OTR (COTR) emissions. Additionally, we suggest that localized transverse structure in the previous self-amplified spontaneous emission (SASE) free-electron laser (FEL) data at APS in the visible-UV regime as reported at FEL02 may be attributed to such beam structure entering the FEL undulators and inducing the SASE at those structures. Separate beam structures 120 microns apart in x and 2.9 nm apart in wavelength were reported. The details of these observations and operational parameters will be presented.

INTRODUCTION

Several years ago the self-amplified spontaneous emission (SASE) free-electron laser (FEL) experiments at the Advanced Photon Source (APS) included a series of observations on z-dependent microbunching as measured by visible light coherent optical transition radiation (COTR) [1-3]. This SASE-induced microbunching exhibited clear spectral effects at the fundamental and second harmonic of the FEL wavelength. The z-dependent gain of the COTR was comparable to that of the SASE as expected. In FEL02 the authors of reference 4 reported localized spatial enhancements of the COTR images, and in fact reported two 250-μm FWHM clusters 120-μm apart and different in wavelength by 2.9 nm in images taken after undulator #6 of a string of 9. At that time it was proposed that there must be localized structures in the electron beam distribution generated perhaps in the chicane that the SASE process selected. Originally, the investigators checked the e-beam emittance with YAG:Ce screens located after the chicane. Some intensity variations of 20% across the profile were seen, but it was not clear these fluctuations were enough to be selected preferentially by the SASE process.

*Work supported by U.S. Department of Energy, Office of Science, Office of High Energy Physics, under Contract No. DE-AC02-06CH11357.

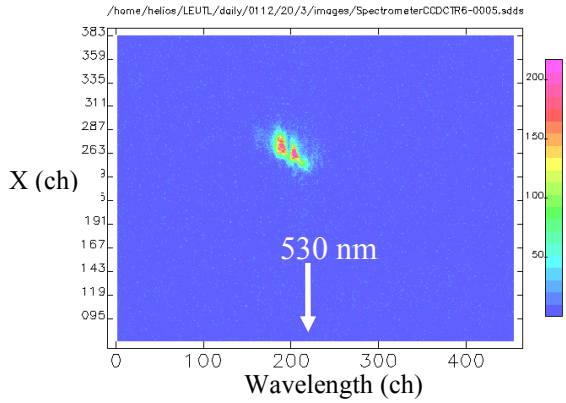

Figure 1: An example of the imaging spectrometer data after undulator 6 showing the COTR x-λ dependence at ~530 nm first reported at FEL02 [4].

As it was understood at that time, there was no theory that supported the coherent synchrotron radiation (CSR) microbunching instability in the linac which could extend to visible wavelengths. We now propose for the first time that the LSC-CSR microbunching instability in the linac at 300-A peak current had induced the observed spatially localized SASE-induced microbunching and related SASE effects in the visible light regime in these 2001 experiments. We report the new evidence for this connection from previously unpublished data. We have reviewed the data taken at an OTR screen just before and after the first undulator, and strong, spatially localized enhancements are clear in the 300-A data! These are comparable to the Fig.1 spatial structures.

More recently, "unexpected" enhancements of the signals in the visible light optical transition radiation (OTR) monitors were observed after compression in a chicane bunch compressor at LCLS and APS [5,6].

EXPERIMENTAL BACKGROUND

The measurements were performed at the APS facility which includes an injector complex with two rf thermionic cathode (TC) guns for injecting an S-band linac that typically accelerates the beam to 325 MeV, the particle accumulator ring (PAR), the booster synchrotron that ramps the energy from 0.325 to 7 GeV in 220 ms, a booster-to-storage-ring transport line (BTS), and the 7-GeV storage ring (SR). In addition, there was an rf photocathode (PC) gun that could also be used to inject into the linac and to ultimately provide beam to the FEL as shown schematically in Fig. 2. An extensive diagnostics suite is available in the chicane and after the chicane area as described in reference 6. The

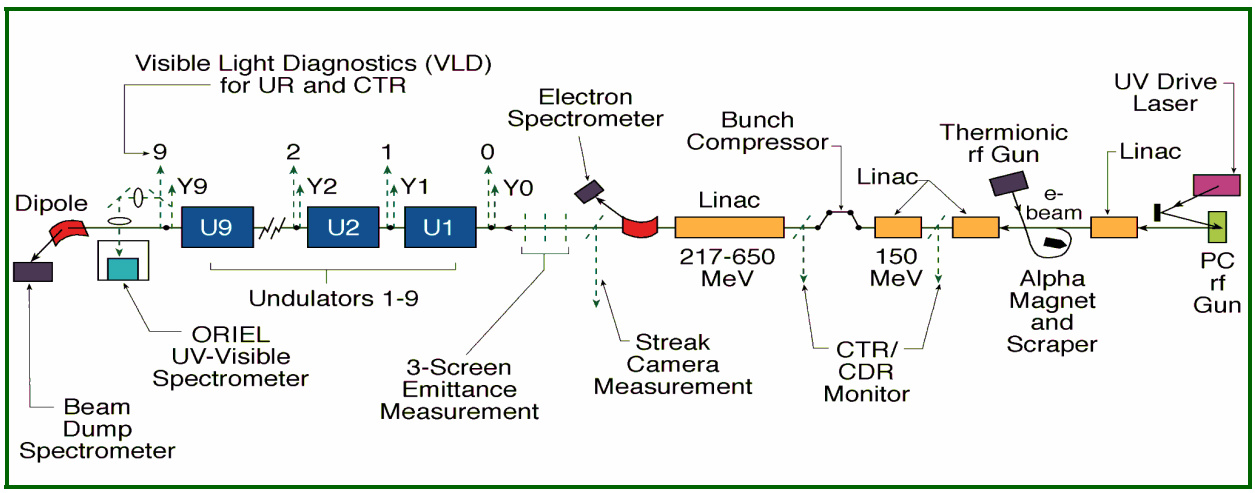

Figure 2: A schematic of the APS linac test area showing the PC rf gun, the TC rf gun, the accelerator structures, the chicane, the decommissioned FEL with VLD stations after each of nine undulators, the imaging optical spectrometer, and the electron beam dump (ref. 4).

microbunching instability tests were performed in the linac at the three imaging stations after the chicane bunch compressor and at the end of the linac where another beam imaging station is located. A FIR coherent transition radiation (CTR) detector (Golay cell) and Michelson interferometer are located between the three-screen emittance stations. This system is described in more detail elsewhere [7].

The YAG:Ce and OTR were directed by turning mirrors and relay optics to a Pulnix CCD camera located 0.5 m from the source. These Chicane stations also have options for low- and high-resolution imaging of the beam spot by selecting one of two lens configurations [8]. The near-field, low-resolution magnification resulted in calibration factors of 48.8 μm per pixel in x and 38.9 μm per pixel in y. The OTR signal strength with a 400-pC micropulse was too low to use the high-resolution mode. The signal intensity was adjusted with a remotely-controlled iris with no absolute position readback) in the path to the camera. The OTR and YAG:Ce images were recorded by a Datacube MV200 video digitizer for both online and offline image analyses, and a video switcher was used to select the camera signal for digitizing.

At the end of the linac, the imaging station included the optical transport of the visible light out of the tunnel to a small, accessible optics lab where the CCD camera was located. This allowed the access for exploring the spectral dependency of the enhanced OTR. A set of bandpass filters with center wavelengths in 50-nm increments from 400 to 700 nm and 40-nm band width as well as a 500-nm shortpass filter and 500-nm long pass filter were used in the initial tests [6]. However, recently the Oriel spectrometer and readout cameras were moved from the FEL hall to this station to extend our spectral analysis capabilities for the LSC-induced COTR effects. The beam energy was 375 MeV at this station in these recent experiments.

The YAG:Ce (Y0-9) and the visible light diagnostics (VLD0-9) stations in the FEL are schematically shown in pairs in Fig. 3. They were designed to assess the z-dependent SASE evolution with both near-field and far-field imaging optics and to track the e-beam position and size through the undulator string. They were augmented to provide an OTR/blocking foil at the first YN actuator. This foil could be used to sort out the SASE and SER from reaching the second retractable pickoff mirror oriented at 45 degrees to the beam direction and 63 mm downstream of the first actuator. This configuration allowed us to do the seminal series of SASE-induced microbunching experiments in the visible regime [1,2] at this downstream portion of the station. The data being reassessed are from a comprehensive set of SASE-induced microbunching tests at two peak currents, 120 A and 300 A, taken on December 20, 2001. The VLD0 station is before the first undulator and provides the key OTR images at the two currents. Evidently the threshold for seeing the LSC-induced microbunching effects in the visible regime was passed at the higher current with 2.5 times more compression.

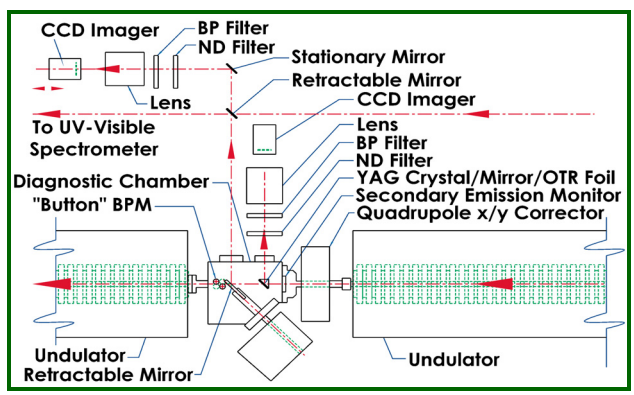

Figure 3: A schematic of the YN and VLD stations located before the first undulator and after each of the nine undulators at the time of the SASE-induced COTR experiments.

RECENT CTR AND COTR RESULTS

The more recent experiments [6] were initiated by transporting the PC gun beam accelerated to 150 MeV to the chicane area. The rf phase of the L2 accelerator structure located before the chicane was used to establish the appropriate conditions for compression in the chicane. The degree of compression was tracked with the Golay cell signals. A very strong variation of the FIR signal with L2 phase was observed. There was almost no signal seen when uncompressed and 300 units seen at the peak compression. The autocorrelation scan was then done and showed a profile width of ~65 μm (FWHM). This would mean a roundtrip time of 130 μm, or about 430 fs (FWHM). The initial PC gun bunch length was 3 to 4 ps (FWHM) as determined by the drive laser pulse.

Having determined we had good compression from the Golay-cell data, we then sampled the beam images at the three screens after the chicane in the emittance measurement area. The sample shown is from FS5, the third screen of the set. At the point of minimum compression the OTR image is weak, but visibly tilted in x-y space. In contrast, the image taken near full compression as indicated by the FIR CTR signal has significantly enhanced localized spikes of about 250 μm (FWHM) spatial extent as shown in Fig. 4. The pseudo-color intensity scale at the right of the image shows that the red areas are high intensity. The profile at the right shows the peak intensity of 180 counts, almost 10 times the adjacent intensities in the beam-image footprint. We do not see the ring-like structure in the enhancement reported at LCLS [5], but we also don't have a harmonic cavity for linearizing longitudinal phase space before the chicane as LCLS has. On this particular run, we noted that there seemed to be a preferred location in the footprint to be enhanced. The enhanced vertical band in Fig. 4 is the same area that shows less enhancement with less compression.

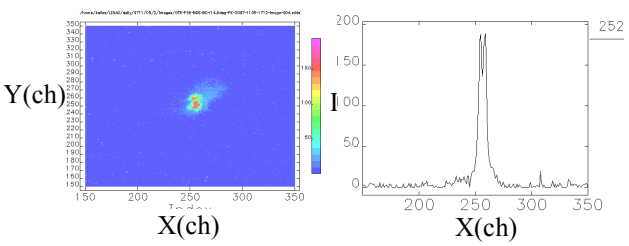

Figure 4: OTR beam image (left) and horizontal profile (right) through spike in distribution after the Chicane with L2 phase = 14.9 degrees, close to maximum compression[6].

An additional indication of the effect is shown in Fig. 5, where the peak intensities from the vertical profiles taken though the images at each phase setting show the rapid increase in the enhanced OTR signal in just a few degrees of L2 phase change. The order of magnitude enhancement is clearly seen in this plot. A similar plot for horizontal profiles was done, and this showed a slight shift of the intensity peak compared to the CTR data by 0.4 degrees in L2 phase. Integrated areas of the ten images at each phase setting do not show this degree of enhancement, but about a 1.6-2 times larger counts integral at peak compression was seen with larger fluctuations in the compressed conditions. This fact is consistent with the premise that the charge transport intensity is not the cause of the effect nor CSR- induced clumping of electrons, but rather a coherent enhancement of some kind is involved.

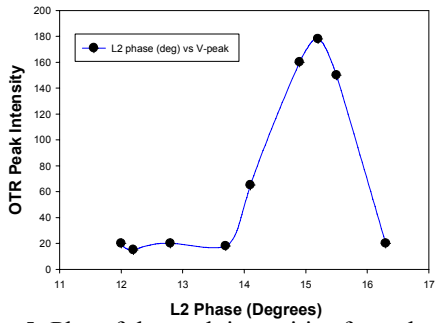

Figure 5: Plot of the peak intensities from the OTR image vertical profiles taken near the enhanced regime coordinates as a function of L2 phase in degrees [6].

In order to assess the spectral dependency of the OTR enhancements, we accelerated the beam to 375 MeV and again imaged the beam spot with OTR at a downstream station. As described previously, this station included transport of the signal outside of the tunnel to a small optics lab. First, we still see enhanced localized spikes when we have compressed the beam as shown in ref.6. In this case enhancements of the OTR signals when at maximum compression are about 3-6 times the normal intensity. The strong fluctuations of these enhanced areas are again suggestive of a coherent process, perhaps seeded by noise.

At full compression we checked the spectral dependency of the enhancements by inserting the bandpass filters in front of the CCD camera. Our preliminary results are that the enhancements were seen at all central wavelengths from 400 to 700 nm (in steps of 50 nm), although relatively weaker in the 400 to 500-nm regime than at 550 nm. We subsequently checked the spectral dependence of incoherent OTR from the TC gun beam and saw a similar intensity rolloff in this short wavelength interval which we attribute to the CCD camera response to these different wavelengths. We also saw more enhancement of intensity in the 500-nm longpass filter than in the 550-nm shortpass filter.

Additionally, in Fig. 6 we show our initial results from the spectrometer when positioned at a station at the end of the linac. The broadband streaks seem to originate from localized x structures which appear with bunch compression. The entrance slit was opened to 2000 μm to facilitate the first data acquisition so the resolution was broadened to about 40 nm. Such post-chicane data are consistent with coherent enhancements of wavelengths longer than a fine longitudinal structure, such as a leading-edge spike. However, a recent report by Z. Huang [9] also shows a broadband enhancement in the visible regime due to the LSC microbunching instability and the

chicane compression process. We suggest now that the discriminating test is that LSC-induced microbunching could induce visible wavelength SASE FELs in a localized spatial–λ manner, and that is consistent with what was actually reported six years ago in the FEL02 transverse dependencies paper [4].

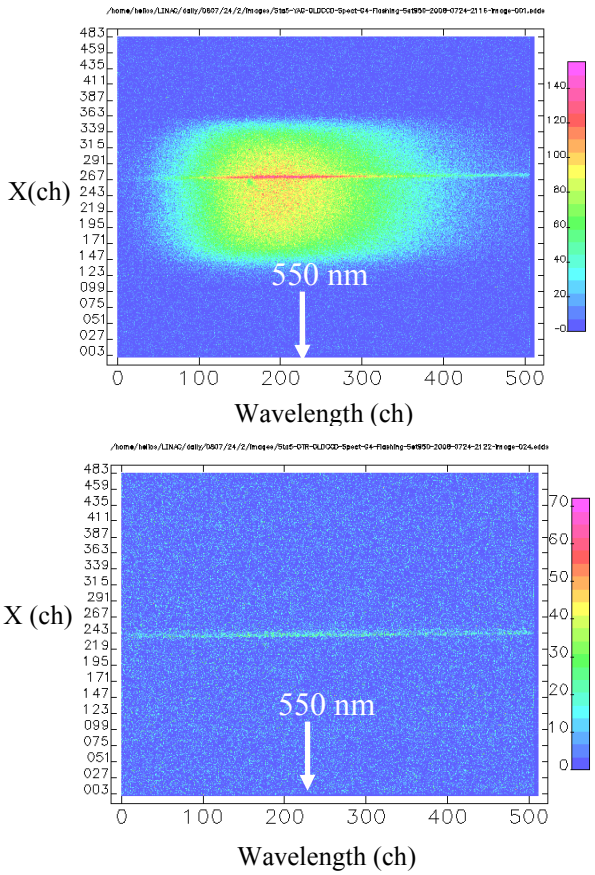

Figure 6: Example x-λ images of the present PC gun beam at 375 MeV near maximum bunch compression for a) YAG:Ce screen plus "COTR streak" and b) the COTR screen only. In this case the 95 lines/mm grating was selected, and the wavelength span is about 180 nm. The broadband emission is clearly from a localized x location.

PAST OTR, COTR, AND SASE RESULTS WITH PC RF GUN BEAMS

The scope of this section is to connect the experimental evidence for enhanced OTR now attributable to LSC-induced microbunching. Our Dec. 2007 COTR data we can now connect with an original series of experiments that were performed on Dec. 20, 2001. The objectives then were to explore the SASE-induced microbunching in the FEL as probed with COTR-based techniques using near-field focusing. In addition, we used a 500-nm short pass filter to exclude the 530-nm fundamental SASE or COTR in the low gain region to check the incoherent broadband image. The beam energy was 217 MeV. Now this filter also lets us look for enhancements that are not SASE induced. In this particular run we only had one filter available with a factor of about 100 rejection ratio for wavelengths longer than 500 nm, so we cannot rely on this to completely reject the SASE-induced contributions after several gain lengths, about undulator 2. We took data at both 120 A and 300 A peak current. The beam parameters are shown in Table 1 in ref. 4. However, the comprehensive test series also included z-dependent gain measurements of both SASE and COTR including the now–critical VLD0 reference data taken just *before the first undulator.* In Fig. 7 we show the beam image from VLD0 at 120 A. It is a relatively weak OTR image with 450 pC of charge. This is compared to a sample image from VLD0 in the 300-A run which clearly has localized spatial enhancements in it as shown in Fig. 8. The same color intensity scale is used, and we added ND 0.5 in the 300-A case. The peaks of Fig. 8 are thus 5-6 times stronger than the 120-A case peak in Fig. 7. The 100-image integrated intensity averages done 6 years ago were 2 times stronger in the 300-A case than the 120-A case for very similar micropulse charge. These results are clear evidence for an enhancement of some kind which we now attribute to the LSC microbunching instability and subsequent COTR emissions.

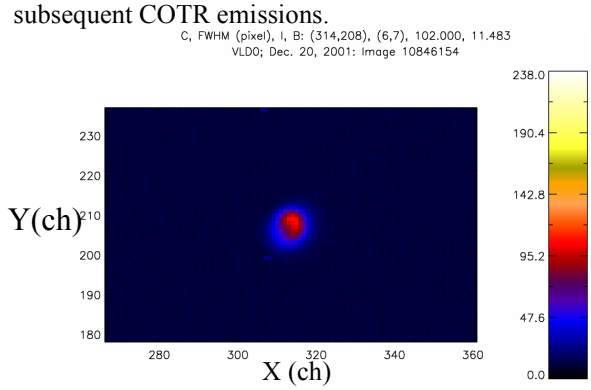

Figure 7: An example of VLD0 OTR data with the 120-A beam and 450-pC micropulse with ND 0.0.

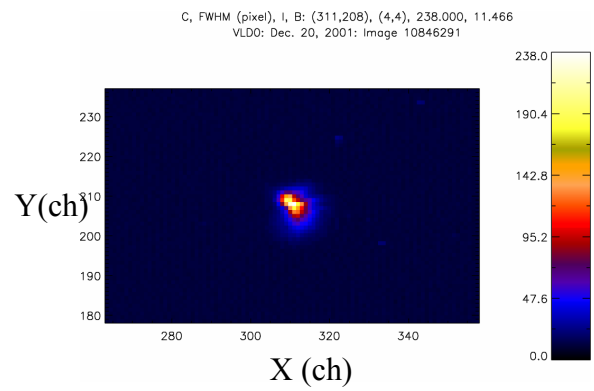

Figure 8: An example of VLD0 OTR/COTR data with the 300-A beam and 450-pC micropulse with ND 0.5.

We then checked that after one undulator the enhancements persist in the 500-nm shortpass data from VLD1 as shown in Fig. 9. Of course, we cannot take simultaneous data sets so this is a different beam micropulse, but the effect remains. The intensity scale on the right provides the factor of 5 ratio of the peaks to base.

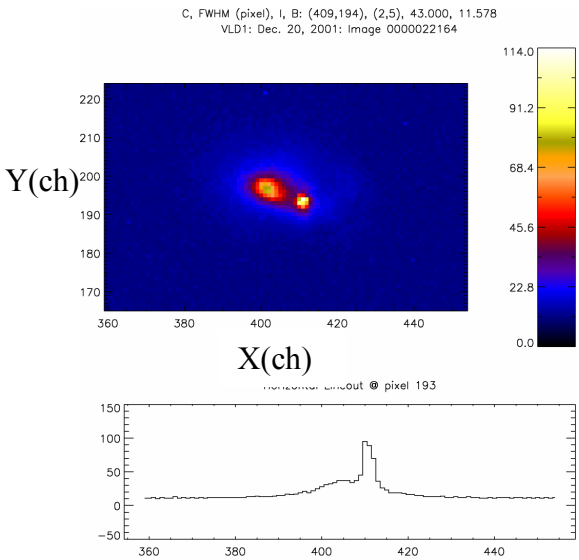

Figure 9: An example of VLD1 OTR/COTR data with the 300-A beam for a 450-pC micropulse. The image is above and the horizontal profile below. The 500-nm shortpass filter blocks any 530-nm SASE-related COTR. There are two distinct peaks shown.

COTR AND SASE: IMAGING SPECTROMETER RESULTS

Having demonstrated that the localized structures are present after VLD0 and VLD1 with 300-A beam, we still need to check that they are also present in the VLD6 data that complement the COTR-6 spectrometer data. In Figs.1,10 we show the x-λ images, one published in FEL02 and one now just being reported. Both of these, as well as many other images taken at that time, show the localized spatial structures. The x-axis is on the vertical display axis. In Fig. 10 the two enhancements are ~150 μm apart in x and ~3 nm apart in wavelength near the nominal 530-nm SASE fundamental wavelength.

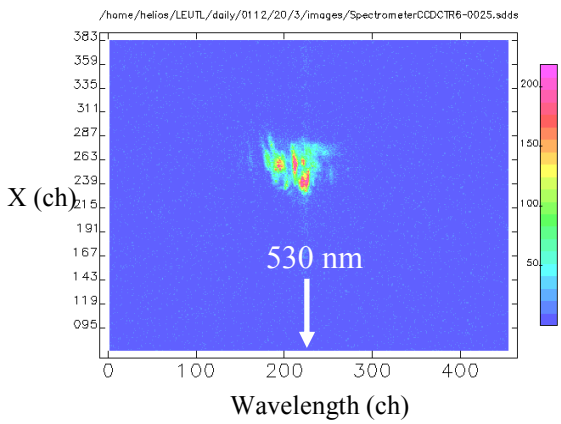

Figure 10: Another example of the imaging spectrometer data showing the COTR x-λ dependence near the 530-nm fundamental wavelength after undulator 6 from Dec. 20, 2001.

Further review of the old data sets led to the finding of the SASE x-λ data shown in Fig. 11.There is structure on the x direction in the vertical display axis. Since physically the spectrometer slit is along this direction, we do not believe this spatial intensity modulation is a diffraction effect from that particular slit. This feature needs additional review of other images and stations.

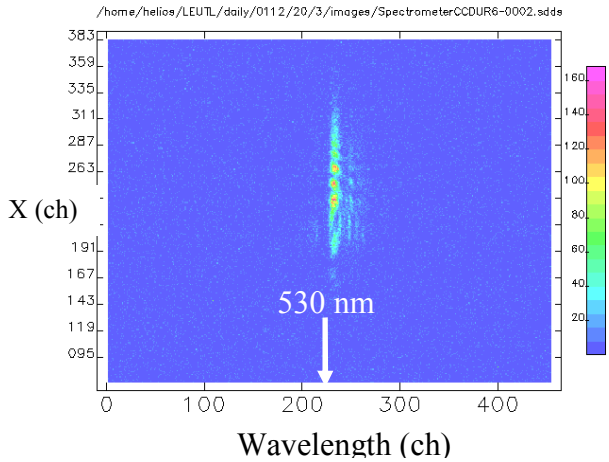

Figure 11: An example imaging spectrometer image of undulator radiation sampled after undulator 6 with the 300-A beam from Dec. 20, 2001. Localized spatial spikes are evident on the vertical display axis which is the x spatial axis.

SUMMARY

In summary, we have connected for the first time the previously reported transverse dependencies on SASE-induced COTR of FEL02 with broadband LSC-induced microbunching effects as identified in investigations described over the last year. This key identification was based on a revisit and interpretation of the 300-A data taken at ANL in 2001, most of which are reported for the first time. Common to these two sets of ANL data are the laser, photocathode material, the linac, the chicane, the optical spectrometer, and some of the investigators. The PC gun cavities are different with quite different transverse emittances, but similar longitudinal emittances. We suggest now that a discriminating factor for LSC-induced microbunching modeling would be whether it induces visible wavelength SASE FELs in a localized spatial–λ manner. This appears consistent with what was actually reported six years ago in the FEL02 transverse dependencies paper [4]. We will be reviewing other data sets from past ANL visible, UV, and VUV SASE experiments as time permits. Start-to-end simulations would be welcomed that investigate this proposed connection. The growing interest in these COTR effects is indicated by the time allowed for discussion in the recent high-brightness beams workshop at Zeuthen in May 2008 [10] and the planned μBI Workshop in October 2008.

ACKNOWLEDGEMENTS

The authors acknowledge support from M. Wendt of Fermilab and R. Gerig and K.-J. Kim of the Argonne Accelerator Institute. We acknowledge discussions with K.-J. Kim, Y.-C. Chae, and M. Borland of Argonne and Z. Huang of SLAC. They also acknowledge W. Berg and S. Shoaf of Argonne for the recent relocation of the optical spectrometer and cameras with controls to the small diagnostics lab linked to linac Sta-5.

REFERENCES

[1] A.H. Lumpkin et al., "First Observation of z-dependent Microbunching using Coherent Transition Radiation," Phys. Rev. Lett., Vol. 86(1), 79, January 1, 2001.

[2] A.H. Lumpkin et al., "First Observations of Micro-bunching 'Sidebands' in a Saturated FEL Using Coherent Optical Transition Radiation", Phys. Rev. Lett., Vol. 88, No. 23, 23480101-1, June 10, 2002.

[3] A.H. Lumpkin et al., "First Observations of Electron-Beam Microbunching in the Ultraviolet At 265 nm Using COTR in a SASE FEL", Nucl. Instr. and Method, A483, 402-406, (2002).

[4] A.H. Lumpkin et al., "Evidence for Transverse Dependencies in COTR and Microbunching in a SASE FEL", the Proc. of the 23rd FEL Conference, Argonne, Il, Sept.9-13, 2002. Nucl. Instr. and Meth. A 507,200-204, (2003).

[5] D.H. Dowell et al., "LCLS Injector Commissioning Results", submitted to Proc. of FEL07, Aug. 26-30, 2007, Novosibirsk.

[6] A.H. Lumpkin et al., "Observations of Enhanced OTR Signals from a Compressed Electron Beam", submitted to the Proc. of BIW08, Tahoe, Ca , May 5-8, 2008

[7] A.H. Lumpkin et al., "Initial measurements of CSR from a Bunch-Compressed Beam at APS." Proc. of FEL05, JACoW/eConf C0508213, 608 (2005).

[8] B. Yang et al., "Design and Upgrade of a Compact Imaging System for the APS Linac Bunch Compressor", BIW2002, AIP Conf. Proc. 648, 393 (2002).

[9] Z. Huang et al., "COTR and CSR from Microbunched LCLS Beam", Mini Workshop on "Characterization of High Brightness Beams," Zeuthen, May 26-30, 2008.

[10] Agenda for Mini Workshop on "Characterization of High Brightness Beams," Zeuthen, May 26-30, 2008.